Journal of
Materials Chemistry C

Accepted Manuscript

Cite this: DOI: 10.1039/c0xx00000x

www.rsc.org/xxxxxx

ARTICLE TYPE

Preparation of 4-dicyanomethylene-2,6-distyryl-4*H*-pyran derivatives, their functional polystyrenes and study of their different aggregation induced emission behaviors

You-Hao Zhang,[a] Pei-Yang Gu,[a] Jie-Bo Zhou,[b] Yu-Jie Xu,[b] Wu Liu,[a] Qian-Feng Gu,[a] Dong-Yun Chen,[a] Na-Jun Li,[a] Qing-Feng Xu,*[a] and Jian-Mei Lu*[a]

Received (in XXX, XXX) Xth XXXXXXXXX 20XX, Accepted Xth XXXXXXXXX 20XX
DOI: 10.1039/b000000x

Red fluorescent materials with efficient light emission in aggregate or solid state are rare but have a wide application in optoelectronic and biological fields. Herein, two pyran derivatives, EtAmPy and EtOxPy with different charge transfer (CT), were designed as initiators and introduced to polystyrene chains *via* atom transfer radical polymerization (ATRP).The emission of EtAmPy was quenched both in high polar solvents and aggregate state because of its strong CT and intermolecular interactions, respectively. After EtAmPy was introduced to normal polystyrene chains, the obtained functional PS emitted strong red light with quantum yield of 37% in aggregate state. Different from EtAmPy, EtOxPy, possessing a weak CT and not sensitive to the change of microenvironment, was AIE-active and displayed a large red shift in emission spectra in aggregate state. Meanwhile, the functional PS initiated by EtOxPy showed obviously blue-shifted emission, compared to its initiator, in aggregate state by reducing their intermolecular interactions. EtAmPy-functionalized polystyrene had a successful application in cell imaging. Therefore, using CT effect in molecular design and polymerization is beneficial to obtaining new red emission probes.

Introduction

The development of luminescent materials with efficient light emission in aggregate or solid state has attracted great attention, due to their potential in organic light-emitting diodes (OLEDs), chemosensors and biolabels.[1-15] Since Professor Tang and coworkers found a novel phenomenon of aggregation-induced emission (AIE) in 2001, which could tackle the aggregation-caused quenching (ACQ) problem not accompanied by severe side effects, many groups have designed, synthesized new AIE-active molecules, and investigated their aggregate morphologies and manipulation of their luminescence.[16-27] To date, materials with efficient red emission in their aggregate or solid state are still rare. Red luminophores are usually polar, such as DCM (4-dicyanomethylene-2,6-distyryl-4H-pyran) or non-polar but extensively π-conjugated, such as TPP(5,10,15,20-teraphenylporphyrin).[28-30] Either attractive dipole-dipole interactions or effective intermolecular π-stacking could quench their emission in aggregate or solid state.[30] One strategy to solve this problem is covalently attaching AIE units such as tetraphenylethene (TPE) to the red luminophores.[32-34] For example, Tang's group has reported a DCM derivative, TPE-TPA-DCM, possessing both AIE and intramolecular charge transfer (CT) features.[35] Its nanoparticles (NPs) exhibit efficient FR/NIR fluorescence, and are applied in bioimaging successfully.[36] Another approach to preserving intramolecular CT effect in AIE systems is the effective wrapping of polar luminophores by polymer chains. Our previous work introduced a single AIE initiator TPP-NI into the end of normal polymer chains such as polystyrene (PS), polymethyl methacrylate (PMMA) and polyhydroxyethyl methacrylate (PHEMA) *via* ATRP and got functional polymers.[37] The dual photoresponse by intramolecular CT and AIE of the initiator is well-realized and even enlarged after polymerization, which indicates that the polymer chains could play an important role in reducing the dipole-dipole interactions between initiators and recover the emission of initiators in aggregate or solid state.[38]

In this paper, we designed and synthesized two pyran derivatives, 2-Bromo-2-methyl-propionic acid 2-{[4-(2-{6-[2-(4-{[2-(2-bromo-2-methyl-propionyloxy)-ethyl]-methyl-amino}-phenyl)-vinyl]-4-dicyanomethylene-4H-pyran-2-yl}-vinyl)-phenyl]-methyl-amino}-ethyl ester (abbreviated as EtAmPy) and 2-Bromo-2-methyl-propionic acid 2-(4-{2-[6-(2-{4-[2-(2-bromo-2-methyl-propion-yloxy)-ethoxy]-phenyl}-vinyl)-4-dicyanomethylene-4H-pyran-2-yl]-vinyl}-phenoxy)-ethyl ester (abbreviated as EtOxPy), and introduced two PS chains to the periphery of initiators *via* ATRP.[39-40] As we know, the electron-donating ability of the substituent in the para position of the styryl units influences the electronic interaction between D-A pairs, and the electron-donating ability of ethyoxyl group is weaker than substituted amino.[41] As a result, CT of EtAmPy is stronger than that of EtOxPy, as well as the intermolecular interactions, which makes a difference to their sensitivity to the change of microenvironment and their optical properties in

solution and aggregate state.[42] On the other hand, the peripheral PS chains could be used as building blocks to reduce the intermolecular interaction between initiators, and hence eliminate the ACQ effect and amplify the aggregation-induced emission. Thus, we have systematically studied the effect of PS chains on the two initiators with different CT, as well as the effect of the chain length on the emission of EtAmPy. Considering the bright red aggregation emission of the functional PS initiated by EtAmPy, we have prepared its NPs by using bovine serum albumin (BSA) as a surfactant and applied it to cell imaging.[43-44]

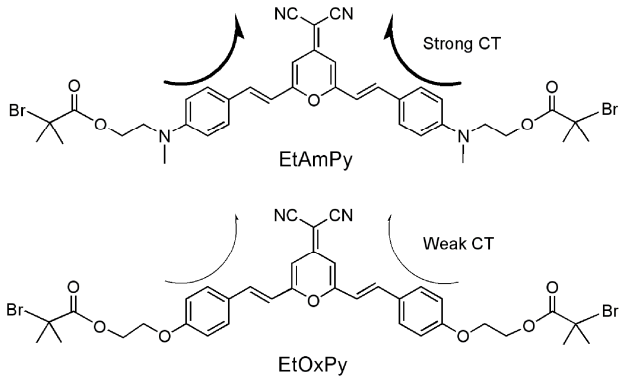

Scheme 1. Molecular structure of EtAmPy and EtOxPy.

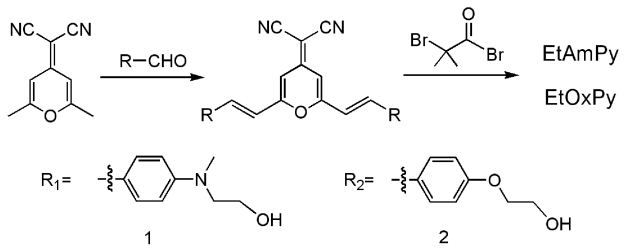

Scheme 2. Synthetic route for EtAmPy and EtOxPy.

Experimental section

Materials

All the materials and reagents were used as purchased without further purification except otherwise stated. 2,6-Dimethyl-γ-pyrone, 2-(methylamino)ethanol, and N,N,N',N',N''-penta-methyl-diethylenetriamine (PMDETA) were purchased from Tokyo Chemical Industry Co., LTD. 4-Fluorobenzaldehyde and 2-bromo-2-methylpropionyl bromide were purchased from Energy Chemical. Malononitrile, 4-hydroxybenzaldehyde, ethylene chlorohydrin, 18-crown-6, potassium carbonate, piperidine, n-propanol, acetic anhydride, triethylamine (TEA), cyclohexanone, copper (I) bromide (CuBr), dimethyl formamide (DMF), dimethyl sulfoxide (DMSO), tetrahydrofuran (THF), chloroform and styrene were purchased from Sinopharm Chemical Reagent. CuBr was purified in acetic acid, washed with ethanol and ether and dried under vacuum to afford a white powder. Cyclohexanone and PMDETA were distilled under vacuum. THF and TEA were dried over appropriate agent and stored over 3 Å molecular sieves before use. Styrene was passed through a short column of aluminium oxide to remove inhibitors prior to polymerization.

General characterization

^{1}H NMR spectra were measured by INOVA 400 MHz NMR spectrometer and ^{13}C NMR spectra were measured by INOVA 300 MHz NMR spectrometer, $CDCl_3$ or DMSO-d_6 as solvent and tetramethylsilane (TMS) as the internal standard at room temperature. Molecular weights and the polydispersity indexes (PDIs) relative to PS were measured using Waters1515 GPC with THF as a mobile phase at a flow rate of 1 mL min^{-1} and with column temperature of 30 ^{o}C. The monomer conversions of polymerization were determined by gravimetric method. UV-vis absorption spectra were determined on a Shimadzu RF540 spectrophotometer using a 1 cm square quartz cell. Room temperature emission spectra were carried out using Edinburgh-920 fluorescence spectra photometer with a slit of 5 cm and the fluorescent quantum yield (Φ_F) in the solution and aggregate states were estimated by using fluorescein (Φ_F = 79% in 0.1 mol L^{-1} NaOH) as standard. SEM images were taken on a Hitachi S-4700 scanning electron microscope. Thermogravimetric analysis (TGA) was conducted on a TA Instruments Dynamic TGA 2950 at a heating rate of 10 ^{o}C min^{-1} and under an N_2 flow rate of 50 mL min^{-1}. Differential scanning calorimetry (DSC) analysis was performed on a Shimadzu DSC860A 85 instrument. Dynamic light scattering (DLS) were carried out at 25 ^{o}C using a Zetasizer Nano-ZS from Malvern Instruments equipped with a 633 nm He–Ne laser using back-scattering detection.

Synthesis of 2-[2,6-bis-(2-{4-[(2-hydroxy-ethyl)-methyl-amino]-phenyl}-vinyl)-pyran-4-ylidene]-malononitrile (1)

2,6-(dimethyl-4H-pyran-4-ylidene)malononitrile (30 mmol, 5.16 g), 4-[(2-hydroxy-ethyl)-methyl-amino]-benzaldehyde (70 mmol, 12.53 g) and 10 drops of piperidine were dissolved in 50 mL of n-propanol and heated to reflux for 24 h. After the complete conversion of 2,6-(dimethyl-4H-pyran-4-ylidene)malononitrile, the reaction mixture was cooled and filtered. The precipitate was washed with 40 mL of ethanol and recrystallized three times from DMF/ethanol mixture (1:10 by volume). Yield: 53% (15.9 mmol, 7.85 g). ^{1}H NMR (400 MHz, DMSO-d_6) δ (ppm) 7.71-7.56 (m, 5H), 7.02 (d, *J = 15.8 Hz*, 2H), 6.76 (d, *J = 8.4 Hz*, 3H), 6.65 (s, 2H), 4.74 (s, 2H), 3.58 (d, *J = 5.6 Hz*, 4H), 3.48 (s, 4H), 3.02 (s, 6H). ^{13}C NMR (300 MHz, DMSO-d_6) δ (ppm) 53.57, 54.36, 58.63, 105.22, 111.94, 113.32, 116.86, 122.56, 130.45, 138.78, 151.13, 156.22, 160.30.

Synthesis of 2-(2,6-bis-{2-[4-(2-hydroxy-ethoxy)-phenyl]-vinyl}-pyran-4-ylidene)-malononitrile (2)

The procedure was similar to that for the preparation of 1. Yield: 55% (16.5 mmol, 7.72 g). ^{1}H NMR (400 MHz, DMSO-d_6) δ (ppm) 7.74 (t, *J = 11.3 Hz*, 6H), 7.25 (d, *J = 16.1 Hz*, 2H), 7.04 (d, *J = 8.2 Hz*, 4H), 6.81 (s, 2H), 4.92 (t, *J = 5.0 Hz*, 2H), 4.06 (s, 4H), 3.74 (d, *J = 4.5 Hz*, 4H). ^{13}C NMR (300 MHz, DMSO-d_6) δ (ppm) 56.16, 59.95, 70.17, 106.70, 115.33, 116.18, 117.03, 128.04, 130.37, 137.91, 156.48, 159.61, 160.88.

Synthesis of EtAmPy

Compound 1 (10 mmol, 4.94 g) and dried TEA (80 mmol, 8.08 g) were dissolved in 200 mL of anhydrous THF and cooled with ice. After the solution was cooled below 0 ^{o}C, 2-bromo-2-methyl propionyl bromide (60 mmol, 13.80 g), dissolved in 20 mL of anhydrous THF, was added dropwise. The mixture was stirred for another hour at 0 ^{o}C and then stirred overnight at room temperature. The reaction mixture was filtered and the filtrate was poured into cold water. The precipitate was filtered and recrystallized twice from ethyl acetate. Yield: 69% (6.9 mmol, 5.46 g). ^{1}H NMR (400 MHz, DMSO-d_6) δ (ppm) 7.70-7.62 (m,

6H), 7.08 (d, *J = 16.0 Hz*, 2H), 6.82 (d, *J = 8.5 Hz*, 4H), 6.69 (s, 2H), 4.32 (s, 4H), 3.77 (s, 4H), 3.04 (s, 6H), 1.81 (s, 12H). ^{13}C NMR (300 MHz, DMSO-d_6) δ (ppm) 30.87, 39.15, 50.35, 54.19, 57.76, 64.22, 105.74, 112.55, 114.16, 117.01, 123.49, 130.68, 138.92, 151.05, 156.57, 160.51, 171.53. m.p.=180 ± 0.5 °C. Anal.Calcd for $C_{38}H_{40}Br_2N_4O_5$: N, 7.07%, C, 57.57%, H, 5.05%; found, N, 7.06%, C, 57.67%, H, 5.13%. LC-MS (*m/z*): $[M + Na]^+$ calcd for $C_{38}H_{40}Br_2N_4NaO_5$, 813.1258; found, 813.1251.

Synthesis of EtOxPy

The procedure was similar to that for the preparation of EtAmPy. Yield: 73% (7.3 mmol, 5.59 g). ^{1}H NMR (400 MHz, DMSO-d_6) δ (ppm) 7.77 (t, *J = 11.6 Hz*, 5H), 7.28 (d, *J = 16.1 Hz*, 2H), 7.09 (d, *J = 8.4 Hz*, 4H), 6.83 (s, 2H), 4.50 (s, 4H), 4.33 (s, 4H), 1.90 (s, 12H). ^{13}C NMR (300 MHz, DMSO-d_6) δ (ppm) 30.92, 56.52, 57.69, 64.86, 66.48, 107.13, 115.81, 116.40, 117.64, 128.78, 130.63, 138.06, 156.81, 159.87, 160.61, 171.50. m.p.=173±0.5 °C. Anal.Calcd for $C_{36}H_{34}Br_2N_2O_7$: N, 3.66%, C, 56.40%, H, 4.44%; found, N, 3.34%, C, 55.84%, H, 4.57%. LC-MS (*m/z*): $[M + Na]^+$ calcd for $C_{36}H_{34}Br_2N_2NaO_7$, 787.0625; found, 787.0622.

Polymer synthesis

All ATRP reactions were carried out following a typical experimental procedure: Initiator (0.02 mmol), CuBr (0.06 mmol, 8.64 mg), PMDETA (0.12 mmol, 20.76 mg), cyclohexanone (1 mL), and styrene (10mmol, 1.04 g) were mixed in a round-bottomed flask. The flask was sealed and cycled four times between vacuum and nitrogen. The polymerization took place at 70 °C for a certain time under a nitrogen atmosphere. Samples, taken at regular intervals using a syringe for conversion and molecular weight analysis, were diluted with THF, passed through a short column of basic aluminium oxide to remove copper ions, and precipitated in a large amount of methanol. The product was filtered and dried under vacuum.

Preparation of BSA NPs loaded with functional PS or EtAmPy

To a solution of BSA (10 mg) in physiological saline (5 mL) was added dropwise 1.3 mL of 1 mg mL^{-1} functional PS (M_n=5320) or EtAmPy in pure THF. The mixture was under vigorous stirring at 25 °C for 24 hours. And then the mixture was evaporated to thoroughly remove the remaining THF on a rotary evaporator under vacuum. The BSA NPs suspension was filtered through a 0.45 μm microfilter and left for 12 hours to stabilize before use.

Result and discussion

Polymer characterization

Polymerizations of styrene were processed by using EtAmPy (or EtOxPy) as initiator, CuBr/PMDETA as a catalyst system, and cyclohexanone as a solvent. A proper ratio was selected: $[initiator]_0:[CuBr]_0:[PMDETA]_0:[styrene]_0$ = 1:3:6:500, $[styrene]_0$ = 10.0 mol L^{-1}. The kinetic plot of polymerization was presented in Figure S1-1. The linearity of the semi-logarithmic plot of $\ln([M]_0/[M])$ versus time indicated that the polymerization was first-order with respect to the monomer and that the concentration of the growing radicals remained constant. The number average molecular weight (M_n) increased linearly with the conversion, and the PDIs of the polymers were relatively narrow in all cases (M_w/M_n = 1.20~1.40) (Figure S1-2, TABLE S1). All of these results suggested that the polymerization was well-controlled.

To study the effect of PS with different chain lengths on the properties of EtAmPy, we chose three polymers with different molecular weights (M_n = 5320, 9220, 14740), and named them PSa, PSb and PSc, respectively. We also synthesized PSd (M_n = 6390, PDI = 1.35) to further research the impact of the PS chains on the properties of EtOxPy with weaker CT.

Thermal stability

The thermal properties of polymers were evaluated by TGA and DSC under nitrogen atmosphere as shown in Figure S9 .The 5% weight-lost temperatures (T_d) of PSa, PSb, PSc and PSd were 298 °C, 324 °C, 333 °C and 326 °C, respectively, and the glass transition temperatures (T_g) of them were found to be 97 °C, 100 °C, 103 °C and 100 °C, respectively.

Solvent effect

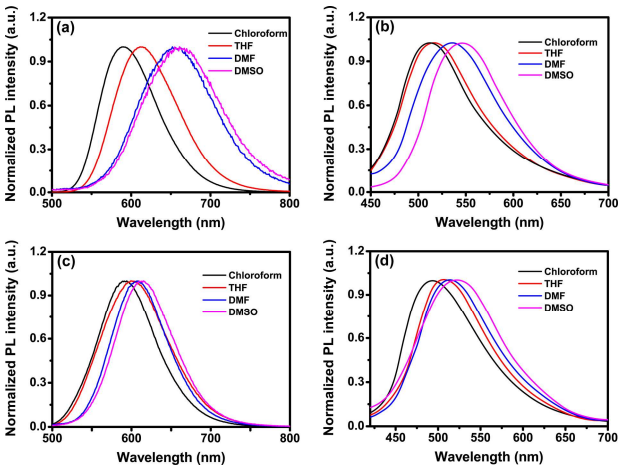

Fig. 1 Emission spectra of (a) EtAmPy and (c) PSa in different polar solvents. Concentration: 10 μM. Excitation wavelength: 479 nm. Emission spectra of (b) EtOxPy and (d) PSd in different polar solvents. Concentration: 10 μM. Excitation wavelength: 415 nm.

EtAmPy is a kind of DCM derivatives with the typical donor-π-acceptor (D-π-A) structure, which exhibits an ultra-fast CT.[30, 45] To confirm the existence of CT in the luminophore, we measured the absorption and emission spectra of EtAmPy in different polar solvents as shown in Figure S10 (a) and Figure 1 (a), respectively. In the DMSO solution, EtAmPy showed multiple absorption bands at 370 nm and 490 nm, which may be deduced to a localized aromatic π–π* transition and CT transition, respectively. When the solvent polarity decreased, the absorption maximum underwent a blue-shift from 484 nm in DMF to 472 nm in chloroform. EtAmPy exhibited very brilliant fluorescence in chloroform (Φ_F = 24.02%) and THF (Φ_F = 17.94%) solution with a maximum emission wavelength at 590nm and 612nm, respectively, while its emission was so weak that it could be hardly observed in highly polar solvents such as DMF (Φ_F = 0.61%) and DMSO (Φ_F = 0.42%). The difference of the emission maxima can be as large as 71 nm. The decreased photoluminancence (PL) intensity may be attributed to the transformation of the excited state from locally excited (LE) state to intramolecular CT state, as the dye's intramolecular CT state was susceptible to various nonradiative quenching processes in highly polar solvents.[46-47] Compared to EtAmPy, the emission maximum and Φ_F of EtOxPy suffered much smaller change when

the solvent polarity increased. The emission maximum underwent a red shift from 514 nm in chloroform to 542 nm in DMSO as shown in Figure 1 (b). The difference of emission maxima of EtOxPy was smaller than that of EtAmPy suggesting the CT of EtOxPy was weaker.[48] The spatial distributions of the highest occupied molecular orbital (HOMO) and the lowest unoccupied molecular orbital (LUMO) levels of the two initiators were shown in Figure S22. The dipole moment of EtAmPy (14.5 Debye) was larger than EtOxPy (12.7 Debye), which could further illustrate the stronger CT of EtAmPy than that of EtOxPy. The emission of EtOxPy in different polar solvents was very weak with a Φ_F below 0.50%, which may be due to the fact that the weak pull-push interaction between ethyoxyl group (donor) and cyano (acceptor) endowed EtOxPy with such a flexible comformation that the phenyl and pyranyl rings may rotate upon the axes of the olefinic double bonds and the dye was nonemissive in dilute solutions.[41]

Table 1: Optical properties of EtAmPy and PSa in different polar solvents[a]

Solvents	λ_{ab}[b] (nm)	λ_{em}[c] (nm)	Φ_F[d] (%)
Chloroform	472[e] / 466[f]	590 / 588	24.02 / 11.74
THF	476 / 471	612 / 603	17.94 / 11.06
DMF	484 / 481	652 / 607	0.61 / 5.49
DMSO	490 / 488	661 / 612	0.42 / 5.02

[a] Concentration: 10 μM. Excitation wavelength: 479 nm. [b] Absorption maximum. [c] Emission maximum. [d] Fluorescent quantum yield estimated using fluorescein (Φ_F = 79% in 0.1 mol L^{-1} NaOH) as standard. [e] Characteristic values of EtAmPy. [f] Characteristic values of PSa.

The absorption and emission spectra of PSa in different polar solvents were measured to confirm the preservation of CT effect in polymers, as shown in Figure S10 (b) and Figure 1 (c). The absorption pattern of PSa was similar to that of its initiator. Although the PL intensity of PSa was gradually weakened with the solvent polarity increasing, the emission was quenched a little in highly polar solvents (DMF and DMSO), which was different from its initiator. Moreover, the difference of emission maximum of PSa in chloroform and DMSO was 24 nm, much smaller than that of EtAmPy. These phenomena may be ascribed to the factor that non-polar PS chain could reduce the polarization of the initiators induced by solvents and hence the intermolecular interaction between initiators and solvents was weakened. In terms of PSd, no obvious difference was exhibited in its emission spectra (Figure 1 (d)) in different polar solvents just like EtOxPy, and the Φ_F values remained unchanged in the neighbourhood of 0.70% because of its weak CT.

Aggregation behaviors

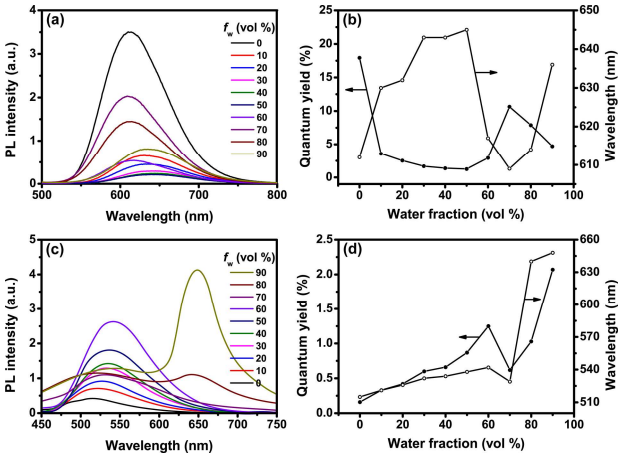

Fig. 2 (a) Emission spectra of EtAmPy in the THF/water mixtures. (b) Plots of quantum yield and maximum wavelength of EtAmPy versus water fraction (f_w) in the THF/water mixture. Concentration: 10 μM. Excitation wavelength: 479 nm. (c) Emission spectra of EtOxPy in the THF/water mixtures. (d) Plots of quantum yield and maximum wavelength of EtOxPy versus water fraction (f_w) in the THF/water mixture. Concentration: 10 μM. Excitation wavelength: 415 nm.

To investigate the aggregation behaviors of EtAmPy, the absorption and PL spectra of the dye in THF/water mixtures with different water fractions were measured and shown in Figure S12 and Figure 2(a). When EtAmPy was molecularly dissolved in pure THF solution, its emission spectrum was peaked at 612 nm with a Φ_F value of 17.94%. The emission was dramatically quenched as f_w in the solvent mixture was progressively increased from 0 to 50%. Meanwhile, the emission maximum was red-shifted to around 645 nm with a Φ_F of 1.26%, which arised from CT effect with the increase of the solvent polarity. When more water was added (f_w > 50 vol %), the solvating power of the mixture was worsened to such an extent that the luminogen molecules began to aggregate. The peak wavelength was blue-shifted to 609 nm in 70% aqueous mixture and the Φ_F value increased to 10.65%, which may be attributed to the factor that the less polar environment inside the nanoaggregates alleviated the CT effect. On the other hand, the formation of aggregate may rigidify and planarize the conformation and extend the conjugation of the dyes. As a result, when f_w reached to 90%, the peak wavelength was red-shifted to 636 nm and the Φ_F value decreased to 4.72%. Moreover, attractive dipole-dipole interaction of polarized EtAmPy dyes facilitated the formation of detrimental excimeric species in the aggregation or solid state, which led to ACQ effect.[36]

Contrary to EtAmPy suffering from ACQ effect, EtOxPy was AIE-active. The emission spectra of EtOxPy in THF/water mixture with different water fractions were shown in Figure 2 (c). When dissolved in pure THF, its emission maximum was at 515 nm with Φ_F as low as 0.16%. When f_w in the solvent mixture was increased from 0 to 60%, its emission was intensified a little with a Φ_F of 1.25% in 60% aqueous mixture. As a large amount of water (f_w > 70%) was added into THF, a level-off tail was observed in the visible region of absorption spectra, indicating the nanosized luminogen aggregates were formed. Unlike EtAmPy, the aggregates of EtOxPy displayed a dual fluorescence emission characterized by a short band at 545 nm and a new long band at 648 nm. With the addition of water, the short band emission

gradually reduced and the long band significantly intensified. Its Φ_F in 90% aqueous mixture was 2.07%, more than 12-fold higher than that of pure THF solution, which was the AIE characteristic. Moreover, the emission maximum underwent a red shift as large as 133 nm from pure THF solution to suspension in 90% aqueous mixture. This may be attributed to the strong intermolecular interactions between EtOxPy molecules after aggregation.[49]

The absorption and emission behaviors were similar for the three PS with different molecular weights. The emission spectra of PSa in THF/water with different water fraction were shown in Figure 3 (a). When dissolved in THF, the absorption maximum was at 471 nm. With the addition of water, the absorption spectra exhibited light-scattering effects in the short band suggesting the formation of aggregates, which was confirmed by SEM (Figure S18). After a "small" amount of water added into THF (f_w < 20%), the PL intensity of PSa was slightly decreased because of the transformation to intramolecular CT state resulting from the gradual increasing polarity of the mixture solvent. After that, the emission was intensified and the emission maximum was progressively blue-shifted to 591 nm (f_w = 90%) due to the weakened microenvironmental polarity near the initiators by aggregated non-polar PS chains. From the molecular solution in pure THF to the aggregate suspension in 90% aqueous solution, the PL intensity enhanced 1.85-fold with a Φ_F increment from 11.06% to 18.50%. It may be attributed to the factor that the aggregated polymer protected the initiators from intermolecular interaction which led to the emission quenching of EtAmPy in aggregate state. Similar results were observed for PSb and PSc, as shown in Figure S14 and Figure S15. The Φ_F values of the three polymers in 90% aqueous suspension are all much higher than those of their pure THF solution (Figure 3 (b)). Evidently, all the three polymers were aggregation-enhanced emission (AEE)-active. More interestingly, as the molecular weights increased, the emission maximum (f_w = 90%) showed a blue-shift to 590 nm and 585 nm for PSb and PSc, respectively. Meanwhile, the aggregate became more emissive, and the Φ_F of PSb and PSc in 90% aqueous solution increased from 22.39% to 37.36%, which further manifested that the longer polymer chains could reduce the probability of the intermolecular interactions between initiators in much higher efficiency.

TABLE 2 Absorption and Emission Characteristics of EtAmPy, EtOxPy, PSa, PSb, PSc, PSd in Solution and Suspension[a]

Sample	λ_{ab}[b] (nm)	λ_{em}[c] (nm)	Φ_F[d] (%)
EtAmPy	476[e]/ 528[f]	612 / 636	17.94 / 4.72
PSa	471 / -[g]	603 / 591	11.06 / 18.50
PSb	468 / -	602 / 590	12.13 / 22.39
PSc	465 / -	594 / 585	16.66 / 37.36
EtOxPy	416 / 422	515 / 648	0.16 / 2.07
PSd	406 / -	508 / 520	0.67 / 4.98

[a] Concentration in solution and suspension: 10 μM. [b] Absorption maximum. [c] Emission maximum. [d] Fluorescent quantum yield estimated using fluorescein (Φ_F = 79% in 0.1 mol L^{-1} NaOH) as standard. [e] Characteristic values in pure THF solvent. [f] Characteristic values in THF/water (1:9, v/v) suspension. [g] Not determined in suspension.

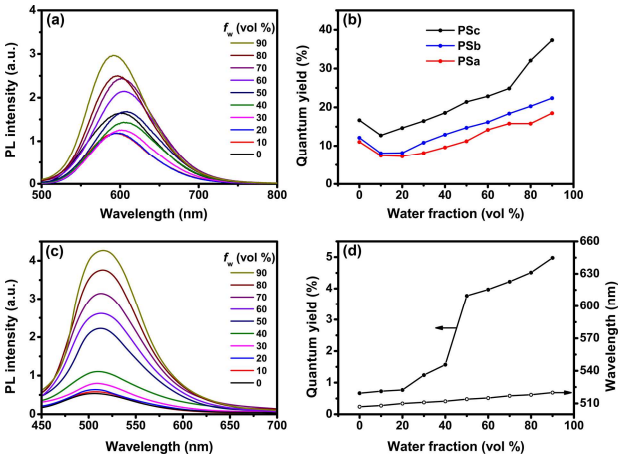

Fig. 3 (a) Emission spectra of PSa in the THF/water mixtures. (b) Plots of quantum yield of PSa, PSb, PSc versus water fraction (f_w) in the THF/water mixtures. Concentration: 10 μM. Excitation wavelength: 479 nm. (c) Emission spectra of PSd in the THF/water mixtures. (d) Plots of quantum yield and maximum wavelength of PSd versus water fraction(f_w) in the THF/water mixtures. Concentration: 10 μM. Excitation wavelength: 415 nm.

To further study the impact of the PS chains on the fluorescent behaviors of EtOxPy whose CT was weaker than EtAmPy, we measured the absorption and emission spectra of PSd in the THF/water mixtures. The absorption pattern of PSd was similar to its initiator. However, the emission of PSd in pure THF solution was peaked at 508 nm with a Φ_F of 0.67%. When the water was added, the emission progressively enhanced and the Φ_F increased to 4.98% in 90% aqueous mixture, accompanying by a slight red shift of 12 nm in the emission maximum. Compared to EtOxPy, the emission spectra of PSd only showed a single short band both in pure THF solution and suspension in THF/water mixtures. The long band at 648 nm of EtOxPy in 90% aqueous mixture did not appear in the emission spectra of PSd. It indicated that the PS chains may functioned as a kind of solid solvent which could separate the initiators from strong intermolecular interactions after aggregation, and restrict intramolecular rotations of the pyranyl and phenyl rings of EtOxPy upon the axes of the olefinic double bonds.[41, 49] Thus, PSd was also AIE-active just like EtOxPy, but only emitted a green light in aggregate state.

Cell imaging

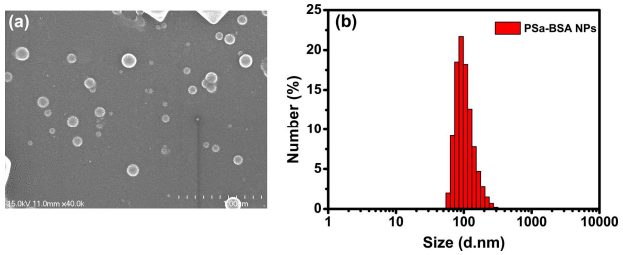

Fig. 4 (a) SEM image of PSa-BSA NPs and (b) size distribution of the particles measured by DLS analysis. Scale bar is 1 μm.

Considering the bright red aggregation emission of PSa, we have prepared its NPs (abbreviated as PSa-BSA NPs) by using BSA as a surfactant. Amphiphilic BSA could interact with PSa through hydrophobic interactions and change the surface to be hydrophilic in aqueous solution. We have also used EtAmPy and BSA to prepare the NPs (abbreviated as EtAmPy-BSA NPs, Figure S20)

at the same condition as we prepared PSa-BSA NPs to compare their difference. As shown in Figure S21 and TABLE S2, the emission of EtAmPy-BSA NPs in physiological saline suspension was almost quenched with a Φ_F value as low as 1.18%. In contrast to EtAmPy-BSA NPs, PSa-BSA NPs emitted bright red aggregation emission whose Φ_F value was as high as 13.34%. Considering this advantage of PSa-BSA NPs, we have applied PSa-BSA NPs to cell imaging. Figure 4 (a) was a SEM image of the obtained PSa-BSA NPs, exhibiting uniform morphology and good monodispersity. The DLS analysis (Figure 4 (b)) also showed that the PSa-BSA NPs had an average diameter of about 146.9 nm and a narrow size distribution (PDI = 0.113), which well corresponded to the SEM result. The potential cell imaging application of the fluorescent PSa-BSA NPs was examined by confocal laser scanning microscope (CLSM) with HeLa cells. The confocal images were taken upon excitation at 488 nm. As shown in Figure 5, bright red fluorescence could be easily observed after cells were incubated with PSa-BSA NPs at 37 ^oC for 3 hours. Apart from the strong fluorescent areas, some dark areas were also found in cells, which could be the location of cell nucleus. These phenomena indicated that the PSa-BSA NPs could be taken up by cells through the nonspecific endocytosis and distribute mainly in the cytoplasm. [50, 51]

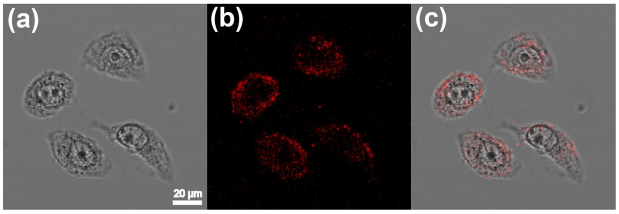

Fig. 5 CLSM images of HeLa cells incubated with BSA NPs at 37 ^oC for 3 hours. (a) Bright field. (b) Excited with 488 nm laser. (c) Overlay of a and b. Scale bar is 20 μm.

Conclusion

In this work, we have synthesized two pyran derivatives with different CT and introduced two PS chains to the periphery of initiators *via* ATRP. EtAmPy, possessing a strong CT, emits a brilliant red light in relatively polar solvents (chloroform and THF), but its emission is quenched in highly polar solvents (DMF and DMSO) and aggregate state because of the CT and ACQ effect, respectively. After introduced to PS chains, the CT of EtAmPy is alleviated by the polymer chains and the emission is "turned-on" in aggregate or solid state. The Φ_F values of the polymers in 90% aqueous suspension are all much higher than those of their pure THF solution. In addition, the longer the polymer chains are, the more enhanced the emission is. Taken advantage of the bright red emission of the functional PS initiated by EtAmPy, its NPs are modified by BSA and applied to cell imaging successfully. Compared to EtAmPy, the CT of EtOxPy is much weaker. It exhibits the typical AIE phenomenon with a red shift as large as 133 nm in emission spectra due to the intermolecular interactions between the dye molecules in aggregate state. However, the PS chains could separate EtOxPy from intermolecular interactions and restrict their intramolecular rotations. As a result, the functional polymer becomes emissive in aggregate state. In summary, we have successfully utilized the polymer chains to tune the optical properties of the luminophores, and studied the interaction between the polymer chains and initiators with different CT.

Acknowledgements

The authors graciously thank the Chinese Natural Science Foundation (21071105, 21371128 and 21336005), Chinese-Singapore Joint Project (2012DFG41900), the Specialized Research Fund for the Doctoral Program of Higher Education of China (grant no. 20113201130003).

Notes and references

[a] *College of Chemistry, Chemical Engineering and Materials Science, Collaborative Innovation Center of Suzhou Nano Science and Technology, Soochow University, Suzhou, 215123, China. E -mail: lujm@suda.edu.cn; xuqingfeng@suda.edu.cn; Fax: +86 0512 65880367; Tel: +86 0512 65880368*

[b] *School of Radiation Medicine and Protection, Soochow University, Suzhou, 215123, China.*

† Electronic Supplementary Information (ESI) available. See DOI: 10.1039/b000000x/

1 M. Sameiro T. Goncalves, *Chem. Rev.*, 2009, **109**, 190.
2 Y. Suzuki, K.Yokoyama, *J. Am. Chem. Soc.*, 2005, **127**, 17799.
3 Y. H. Li, Y. Q. Wu, J. Chang, M. Chen, R. Liu and F. Y. Li, *Chem. Commun.*, 2013, **49**, 11335.
4 M. Faisal, Y. Hong, J. Liu, Y. Yu, J. W. Y. Lam, A. J. Qin, P. Lu and B. Z. Tang, *Chem. –Eur. J.* , 2010, **16**, 4266.
5 Y. Dong, B. Xu, J. Zhang, X. Tan, L. Wang, J. Chen, H. Lv, S. Wen, B. Li, L. Ye, B. Zou and W. Tian, *Angew. Chem. Int. Ed.*, 2012, **51**, 10782.
6 Z. Luo, X. Yuan, Y. Yu, Q. Zhang, D. T. Leong, J. Y. Lee and J. Xie, *J. Am. Chem. Soc.*, 2012, **134** , 16662.
7 Y. Kubota, S. Tanaka, K. Funabiki and M. Matsui, *Org. Lett.*, 2012, **14**, 4682.
8 T. He, X. Tao, J. Yang, D. Guo, H. Xia, J. Jia and M. Jiang, *Chem. Commun.*, 2011, **47**, 2907.
9 Y. Liu, Z. Wang, G. Zhang, W. Zhang, D. Zhang and X. Jiang, *Analyst*, 2012, **137** , 4654.
10 V. Bhalla, A. Gupta and M. Kumar, *Org. Lett.*, 2012, **14**, 3112.
11 A. J. Qin, J. W. Y. Lam and B. Z. Tang, *Chem. Soc. Rev.*, 2010, **39**, 2522.
12 A. J. Qin, J. W. Y. Lam and B. Z. Tang, *Macromolecules*, 2010, **43**, 8693.
13 S. Mukherjee and P. Thilagar, *Chem. Commun.*, 2013, **49**, 7292.
14 J. F. Sun, Y. Lu, L. Wang, D. D. Cheng, Y. J. Sun and X. S. Zeng, *Polym. Chem.*, 2013, **4**, 4045.
15 A. Qin, J. W. Y. Lam and B. Z. Tang, *Prog. Polym. Sci.*, 2012, **37**, 182.
16 Y. N. Hong, J. W. Y. Lam and B. Z. Tang, *Chem. Soc. Rev.*, 2011, **40**, 5361.
17 S. J. Yoon, J. W. Chung, J. Gierschner, K. S. Kim, M. G. Choi, D. H. Kim and S. Y. Park, *J. Am. Chem. Soc.*, 2010, **132**, 13675.
18 B. K. An, S. K. Kwon, S. D. Jung and S. Y. Park, *J. Am. Chem. Soc.*, 2002, **124**, 14410.
19 Y. Liu, X. T. Tao, F. Z. Wang, J. H. Shi, J. L. Sun, W. T. Yu, Y. Ren, D. C. Zou and M. H. Jiang, *J. Phys. Chem. C*, 2007, **111**, 6544.
20 Y. Liu, X. T. Tao, F. Z. Wang, X. N. Dang, D. C. Zou,Y. Ren and M. H. Jiang, *J. Phys. Chem. C*, 2008, **112**, 3975.
21 Z. G. Chi, X. Q. Zhang, B. J. Xu, X. Zhou, C. P. Ma, Y. Zhang, S. W. Liu and J. R. Xu, *Chem. Soc. Rev.*, 2012, **41**, 3878.
22 B. Chen, G. Yu, X. Li, Y. B. Ding, C. Wang, Z. W. Liu and Y. S. Xie, *J. Mater. Chem. C*, 2013, **1**, 7409.
23 G. F. Zhang, M. P. Aldred, W. L. Gong, C. Li and M. Q. Zhu, *Chem.Commun.*, 2012, **48**, 7711.
24 F. F. Wang, J. Y. Wen, L. Y. Huang, J. J. Huang and J. Ouyang, *Chem.Commun.*, 2012, **48**, 7395.
25 Q. Zeng, Z. Li, Y. Q. Dong, C. A. Di, A. J. Qin, Y. N. Hong, L. Ji, Z. C. Zhu, C. K. W. Jim, G. Yu, Q. Q. Li, Z. A. Li, Y. Q. Liu, J. G. Qin and B. Z. Tang, *Chem. Commun.*, 2007, 70.
26 X. J. Diao, W. Li, J. Yu, X. J. Wang, X. J. Zhang, Y. L. Yang, F. F. An, Z. Liu and X. H. Zhang, *Nanoscale*, 2012, **4**, 5373.

27 Z. L. Wang, B. Xu, L. Zhang, J. B. Zhang, T. H. Ma, J. B. Zhang, X. Q. Fu and W. J. Tian, *Nanoscale*, 2013, **5**, 2065.
28 C. T. Chen, *Chem. Mater.*, 2004, **16**, 4389.
29 M. Vanjinathan, H. C. Lin and A. S. Nasar, *J. Polym. Sci., Part A: Polym. Chem.*, 2012, **50**, 3806.
30 Z. Q. Guo, W. H. Zhu and H. Tian, *Chem. Commun.*, 2012, **48**, 6073.
31 B. J. Jung, J. I. Lee, H. Y. Chu, L. M. Do, J. Lee and H. K. Shim, *J. Mater. Chem.*, 2005, **15**, 2470.
32 W. Z. Yuan, P. Lu, S. M. Chen, J. W. Y. Lam, Z. M. Wang, Y. Liu, H. S. Kwok, Y. G. Ma and B. Z. Tang, *Adv. Mater.*, 2010, **22**, 2159.
33 Z. J. Zhao, P. Lu, J. W. Y. Lam, Z. M. Wang, C. Y. K. Chan, H. H. Y. Sung, I. D. Williams, Y. G. Ma and B. Z. Tang, *Chem. Sci.*, 2011, **2**, 672.
34 Z. J. Zhao, S. M. Chen, J. W. Y. Lam, P. Lu, Y. C. Zhong, K. S. Wong, H. S. Kwok and B. Z. Tang, *Chem. Commun.*, 2010, **46**, 2221.
35 J. L. Geng, K. Li, D. Ding, X. H. Zhang, W. Qin, J. Z. Liu, B. T. Tang and B. Liu, *Small*, 2012, **8**, 3655.
36 W. Qin, D. Ding, J. Z. Liu, W. Z. Yuan, Y. Hu, B. Liu and B. Z. Tang, *Adv. Funct. Mater.*, 2012, **22**, 771.
37 P. Y. Gu, C. J. Lu, F. L. Ye, J. F. Ge, Q. F. Xu, Z. J. Hu, N. J. Li and J. M. Lu, *Chem. Commun.*, 2012, **48**, 10234.
38 Y. X. Tao, Q. F. Xu, N. J. Li, J. M. Lu, L. H. Wang and X. W. Xue, *Polymer*, 2011, **52**, 4261.
39 S. H. Lee, M. Ouchi, M. Sawamoto, *J. Polym. Sci., Part A: Polym. Chem.*, 2013, **51**, 4498.
40 K. Nakatani, K. Terashima, M. Ouchi, M. Sawamoto, *Macromolecules*, 2010, **43**, 8910.
41 H. Tong, Y. N. Hong, Y. Q. Dong, Y. Ren, M. Haussler, J. W. Y. Lam, K. S, Wong and B. Z. Tang, *J. Phys. Chem. B*, 2007, **111**, 2000.
42 S. Hecht and J. M. J. Frechet, *Angew. Chem. Int. Ed.*, 2001, **40**, 74.
43 J. Liu, D. Ding, J. L. Geng and B. Liu, *Polym. Chem.*, 2012, **3**, 1567.
44 X. Q. Zhang, X. Y. Zhang, S. Q. Wang, M. Y. Liu, L. Tao and Y. Wei, *Nanoscale*, 2013, **5**, 147.
45 X. F. Xu, R. Q. Zhang, Z. X. Cao and Q. E. Zhang, *J. Theor. Comput. Chem.*, 2008, **7**, 719.
46 R. R. Hu, E. Lager, A. Aguilar-Aguilar, J. Z. Liu, J. W. Y. Lam, H. H. Y. Sung, I. D. Williams, Y. C. Zhong, K. S. Wong, E. Pena-Cabrera and B. Z. Tang, *J. Phys. Chem. C*, 2009, **113**, 15845.
47 M. Mao, M. G. Ren and Q. H. Song, *Chem. Eur. J*, 2012, **18**, 15512.
48 K. Y. Jung and Y. S. Kim, *Mol. Cryst. Liq. Cryst.*, 2011, **538**, 45.
49 H. Tong, Y. Q. Dong, Y. Ren, M. Haussler, Y. N. Hong, J. W. Y. Lam, H. H. Y. Sung, I. D. Williams, H.S. KwoK and B. Z. Tang, *Chem. Phys. Lett.*, 2006, **428**, 326.
50 X. Y. Zhang, X. Q. Zhang, B. Yang, M. Y. Liu,W. Y. Liu, Y. W. Chen and Y. Wei, *Polym. Chem.*, 2013, **4**, 4317.
51 X. Q. Zhang, M. Y. Liu, B. Yang, X. Y. Zhang, Z. G. Chi, S. W. Liu, J. R. Xu and Y. Wei, *Polym. Chem.*, 2013, **4**, 5060.